energies

MDPI

Article

Fuzzy Logic Controller Equilibrium Base to Enhance AGC System Performance with Renewable Energy Disturbances

Soha Mansour [1], Ahmed O. Badr [1], Mahmoud A. Attia [1], Mariam A. Sameh [2], Hossam Kotb [3], Elmazeg Elgamli [4,*] and Mokhtar Shouran [4]

[1] Department of Electrical Power and Machines, Faculty of Engineering, Ain Shams University, Cairo 11517, Egypt
[2] Electrical Engineering Department, Faculty of Engineering, Future University in Egypt, Cairo 11835, Egypt
[3] Department of Electrical Power and Machines, Faculty of Engineering, Alexandria University, Alexandria 21544, Egypt
[4] School of Engineering, Cardiff University, Cardiff CF24 3AA, UK
* Correspondence: elgamlies@cardiff.ac.uk

Abstract: Owing to the various sources of complexity in the electrical power system, such as integrating intermittent renewable energy resources and widely spread nonlinear power system components, which result in sudden changes in the power system operating conditions, the conventional PID controller fails to track such dynamic challenges to mitigate the frequency deviation problem. Thus, in this paper, a fuzzy PI controller is proposed to enhance the automatic generation control system (AGC) against step disturbance, dynamic disturbance, and wind energy disturbance in a single area system. The proposed controller is initialized by using Equilibrium Optimization and proved its superiority through comparison with a classical PI optimized base. Results show that the fuzzy PI controller can reduce the peak-to-peak deviation in the frequency by 30–59% under wind disturbance, compared to a classical PI optimized base. Moreover, a fuzzy PID controller is also proposed and EO initialized in this paper to compare with the PIDA optimized by several techniques in the two-area system. Results show that the fuzzy PID controller can reduce the peak-to-peak deviation in the frequency of area 1 by 30–50% and the deviation of frequency in area 2 by 13–48% under wave disturbance, compared to the classical PIDA optimized base.

Keywords: fuzzy logic controller; equilibrium base; automatic generation control; renewable energy

Citation: Mansour, S.; Badr, A.O.; Attia, M.A.; Sameh, M.A.; Kotb, H.; Elgamli, E.; Shouran, M. Fuzzy Logic Controller Equilibrium Base to Enhance AGC System Performance with Renewable Energy Disturbances. *Energies* **2022**, *15*, 6709. https://doi.org/10.3390/en15186709

Academic Editor: Oscar Barambones

Received: 13 August 2022
Accepted: 8 September 2022
Published: 14 September 2022

1. Introduction

Recently, the power system is becoming more complex due to the integration of renewable energy sources used by the continuous change in generated power, as well as the constant rise in load demand and the variety of generating unit sizes. Moreover, one of the main complex characteristics of the power system is the local and global interconnection of power systems. These interconnections are made through inter-power lines, which are very crucial for the power interchange between different control areas. To maintain the maximum reliability and quality of the power system, the frequency and voltages are mainly monitored and regulated. Two different types of control approaches are mainly used. One is the automatic voltage regulator (AVR), and the other is the automatic generation control (AGC). The AVR system aims to maintain the alternator's output voltage at its supposed value as well as reduce any expected variations in its value if exposed to a fault or unusual condition. To achieve such an objective, AVR controls the exciter's DC current, which is connected to the alternator's rotor, and this is quite an effective approach [1–5]. AGC is another method used to stabilize the frequency tie-line power for various control areas as well as to maintain power balance [6]. Both approaches are very effective. However, some researchers prefer the AGC approach since it includes the effect of interconnected areas, which is more likely to become a real case. Moreover, AGC plays a very essential role in

electric power operation by maintaining the frequency and efficiency of the interconnected power systems [7–11]. Several parameters can be used to control the frequency. One of them is the governor droop (R), which is used to minimize the frequency's steady-state error when it is set to a specified limit, as mentioned in [12–15]. Subsequently, it is a great necessity to have a well-designed controller for AGC. According to [16], there are various control techniques that are used in AGC. They are classified into two classes: one is nature-inspired metaheuristic techniques, and the other is robust control methods. Various metaheuristic algorithms are employed to design the proper controller, such as genetic algorithm (GA), particle swarm optimization (PSO), differential evaluation (DE), ant colony optimization (ACO), and firefly algorithm (FA) [17–21]. They are preferred over other control techniques due to their high accuracy and fast response. The PI controller is very prevalent, due to its high availability in the industry. Therefore, it can be used if its gains are properly chosen. Various optimization algorithms are used for tuning the gains of the PI controller in AGC [22–28]. Furthermore, renewable energy sources are included in [29–32]. The control of AGC is generally studied for single or multi-area systems, as in [33–35]. Fuzzy logic controllers are proposed in [36–38]. Other controllers were proposed in [39–41].

In this paper, the fuzzy logic PI controller with Equilibrium Optimizer (EO) initialization is used in AGC with and without the inclusion of a wind generator in a single area system and is compared with a classical optimized PI controller. Moreover, the fuzzy logic PID controller with Equilibrium Optimizer (EO) initialization is used in a two-area system under step and wave energy disturbance and compared with the optimized PIDA controller. The strategy of the proposed controller is to initialize the PI/PID controller gains by using EO optimization then the fuzzy logic controller will update these gains to deal with the input disturbances.

2. System Modeling

Since the frequency is a key indicator of the robustness of the power system, an efficient load frequency control (LFC) is required to maintain the frequency at its nominal level. Automatic generation control or AGC is a scheme used to regulate the system frequency. The presented systems under study are single-area and two-area systems, as shown in Figure 1. The main components of the system are the governor, the turbine, the generator, the load, and a wind turbine to represent the dynamic disturbances imposed on the system [42], which are explained in the following subsections. In the single-area system, a fuzzy PI controller is presented and compared with the classical optimized-based PI controllers, while in the two-area system, a fuzzy PID controller is presented and compared with the classical optimized-based PIDA controllers.

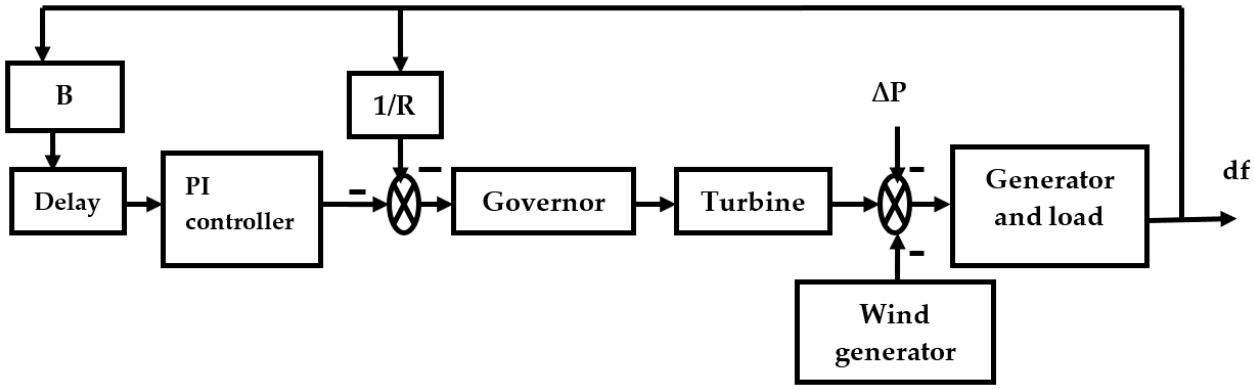

(**a**)

Figure 1. *Cont.*

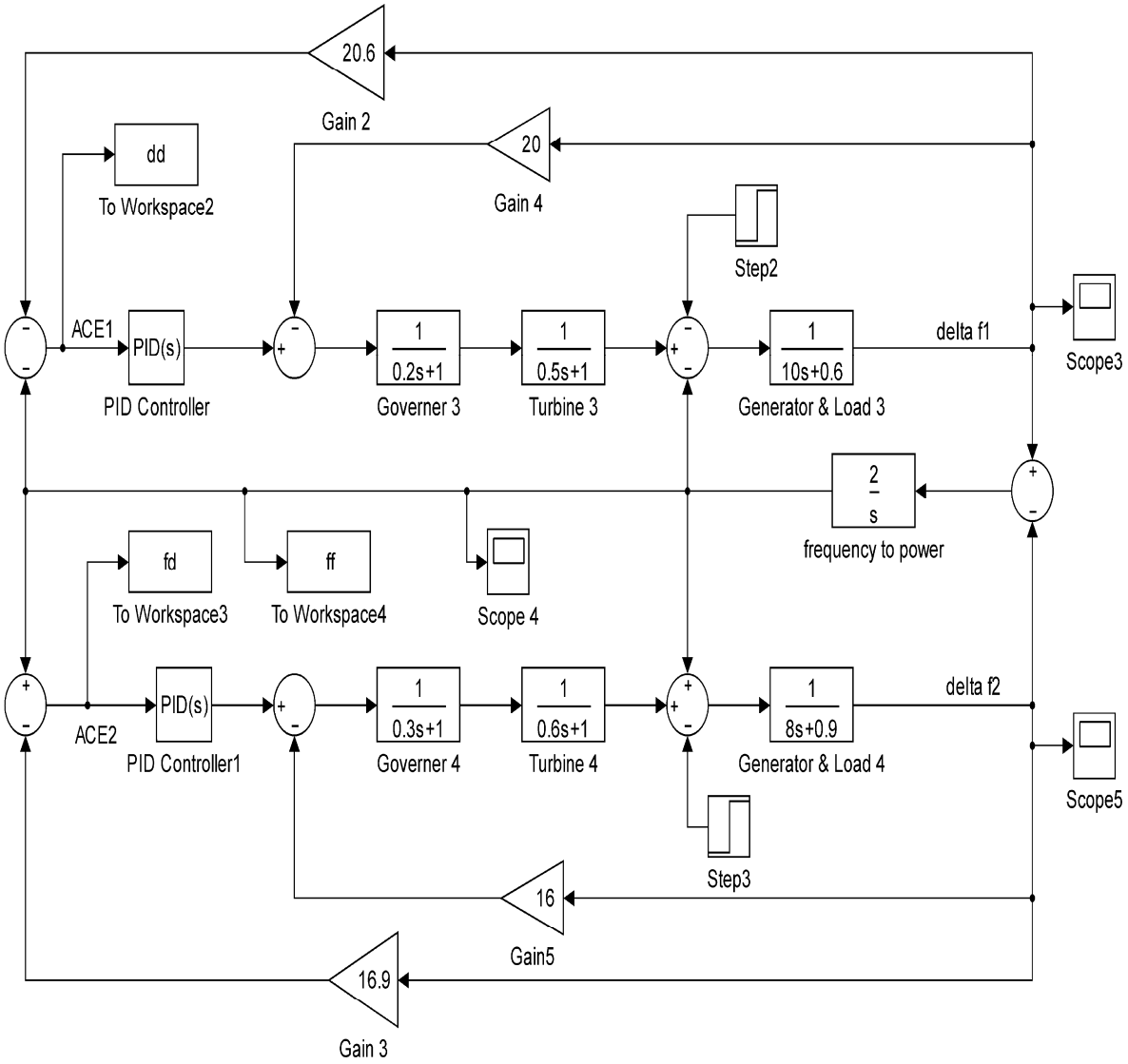

(**b**)

Figure 1. (**a**). Single-area AGC dynamic model and (**b**). Two-area system.

2.1. Governor Model

The governor model is represented using a first-order linear transfer function $\frac{1}{1+sT_g}$ where T_g is the governor time constant.

2.2. Turbine Model

The turbine model is represented by a first-order linear transfer function $\frac{1}{1+sT_{ch}}$ where T_{ch} is the turbine time constant.

2.3. Generator/Load Model

The generator/load model is represented by a first-order linear transfer function $\frac{1}{M_s+D}$ and $B = \frac{1}{R}$ where D is the frequency sensitive coefficient, M is the constant of inertia, R and is the speed regulation, and B is the frequency bias factor.

2.4. Wind Disturbance Generator Model

The mechanically generated output power from the wind turbine generator is represented by the Equation (1):

$$P_{wind} = \frac{1}{2} \times \rho \times C_p \times A \times U^3 \quad (1)$$

where ρ is the flowing air density in kg/m^3, C_p is the power coefficient, A is the swept area in m^2, and U is the wind speed in m/s. The variation in wind speed against time is shown in Figure 2 [42].

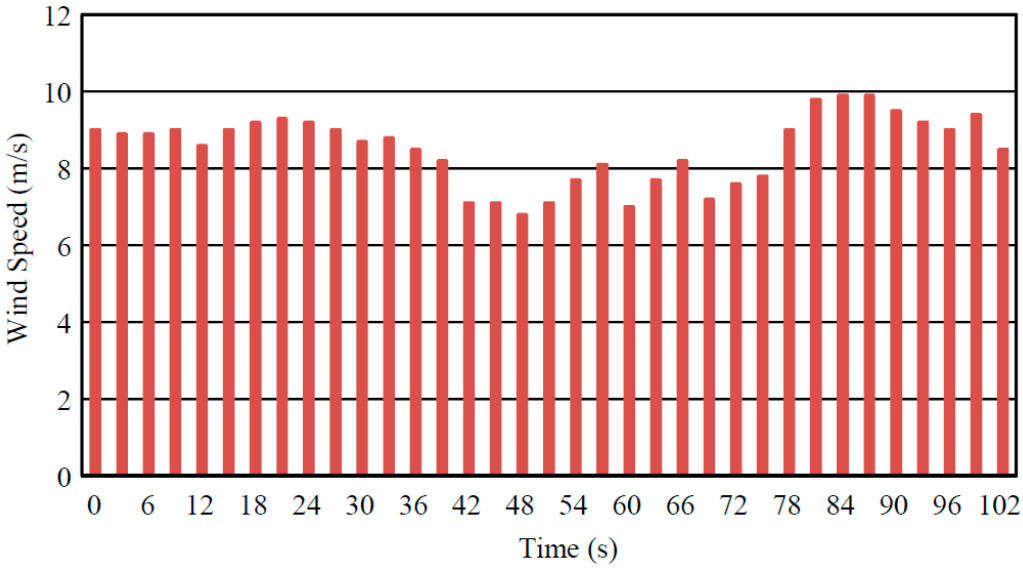

Figure 2. Wind speed profile.

2.5. Proportional Integral Controller Model

A PI controller is employed for providing the control signal to adequately adjust the frequency at its predetermined level. Its transfer function is represented by

$$G(s) = K_p + K_I s \quad (2)$$

An exponential time delay in the single-area system whose time constant equals 2 s is added. The system parameters' values are indicated in Table 1 [27].

Table 1. System parameters.

Symbol	Description	Value
R	speed regulation	0.05
D	frequency sensitive coefficient	1
B	frequency bias factor	21
T_{ch}	turbine time constant	0.3 s
T_g	governor time constant	0.1 s
M	constant of inertia	10 s
C_p	power coefficient	0.5
A	swept area	5538.96 m^2

3. Optimization Algorithms

There are several optimization algorithms that proved their effectiveness. In this study, the authors chose to use an optimization algorithm named the Equilibrium Optimizer (EO) for optimizing the proposed controller due to its high exploitation rate, fast convergence, and high accuracy.

3.1. Equilibrium Optimizer (EO)

Afshin Faramarzi developed a relatively new optimization algorithm in 2020. This algorithm is called the Equilibrium Optimizer algorithm (EO) [43]. The inspiration for this algorithm is performed by the balance models of control between volume and mass. These balance models are used to estimate dynamic and equilibrium states. Most metaheuristic algorithms usually have the same approach. A vector of suggested solutions is primarily generated, then the main algorithm function is used to update the solution vector every iteration. For EO, the volume equilibrium concentration parameter ($\vec{VC}$) is calculated for each suggested solution for updating every iteration. $\vec{VC}$ can be determined from Equation (3) as follows.

$$\vec{VC} = \vec{VC_{eq}} + (\vec{VC} - \vec{VC_{eq}}) \cdot \vec{F} + \frac{\vec{m_g}}{\vec{\alpha} V}\left(1 - \vec{F}\right) \tag{3}$$

Given that:

$\vec{VC}$ is the concentration inside the volume;
V is the volume;
$\vec{VC_{eq}}$ is the concentration at an equilibrium state;
$\vec{m_g}$ is the mass generation rate;
$\vec{\alpha}$ is the turnover rate, it is assumed to be a random vector in the interval of [0, 1];

While $\vec{F}$ can be calculated using Equation (4) as follows:

$$\vec{F} = s_1 \, sign\left(\vec{\sigma} - 0.5\right)\left[e^{-\vec{\alpha} t} - 1\right] \tag{4}$$

Known that:

s_1 is a constant value that control the exploration ability. It equals to 2;
$\vec{\sigma}$ is a random vector in the interval of [0, 1].

Moreover, it is time defined in terms of running iteration (I) and the maximum number of iterations (I_m) and diminishes with the number of iterations. It can be determined from Equation (5).

$$t = \left(1 - \frac{I}{I_m}\right)^{\left(s_2 \frac{I}{I_m}\right)} \tag{5}$$

where $\vec{m_g}$ can be determined from Equation (6), while $\vec{m_{gi}}$, t_o, and P_g are calculated from Equations (7)–(9), respectively.

$$\vec{m_g} = \vec{m_{gi}} \, e^{-\vec{\alpha}(t - t_o)} = \vec{m_{gi}} \, \vec{F} \tag{6}$$

$$\vec{t_o} = \frac{1}{\alpha} ln\left(-s_1 \, sign\left(\sigma - 0.5\right)\left[1 - e^{-\alpha t}\right]\right) + t \tag{7}$$

$$\vec{m_{gi}} = \vec{C_p}(\vec{VC_{eq}} - \alpha \vec{VC}) \tag{8}$$

$$\vec{R_v} \begin{cases} 0.5\omega_1 & \omega_2 \geq P_g \\ 0 & \omega_2 < P_g \end{cases} \tag{9}$$

Note that,

ω_1 and ω_2 are random numbers in the interval of [0, 1];
$\vec{R_v}$ is a vector constructed by the repetition;
P_g is the generation probability.

EO is used to optimize the PI/PID controller gains, and the flowchart in Figure 3 shows how it is used in this case [43].

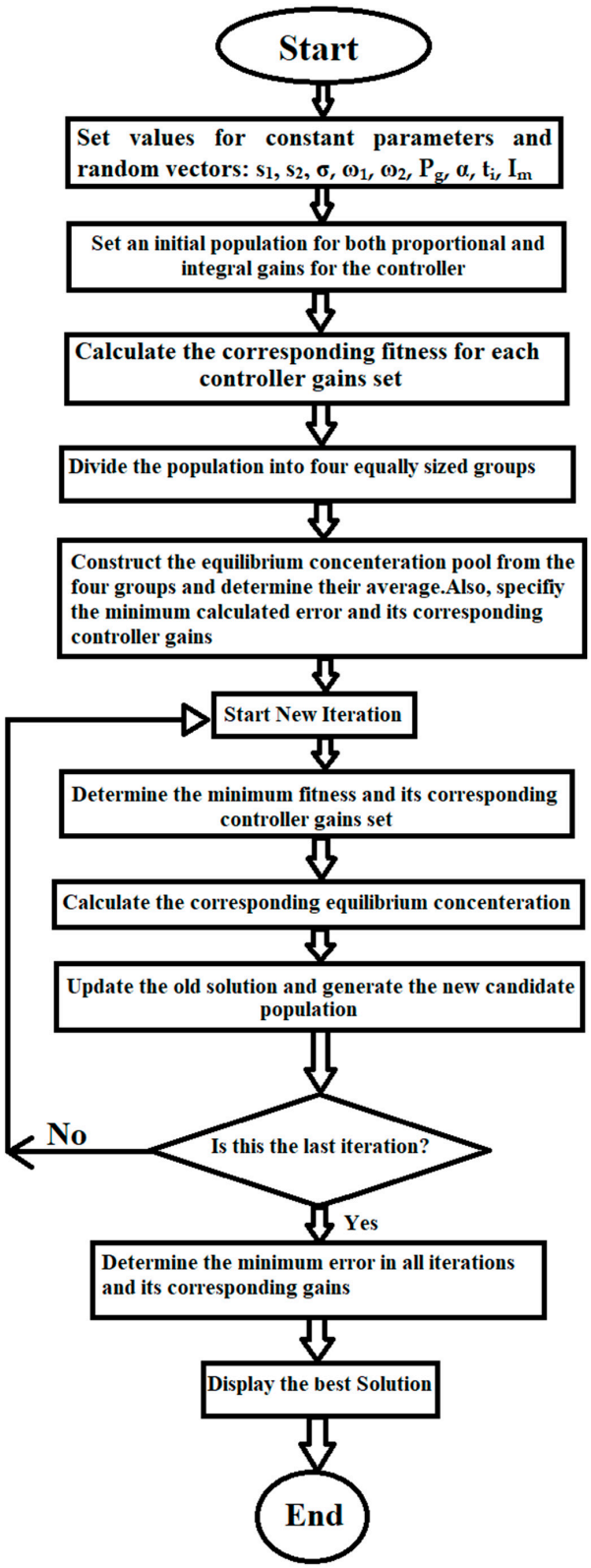

Figure 3. Flowchart of EO algorithm.

3.2. Fuzzy EO PID/PI Controller

The fuzzy control technique was applied successfully as a soft computing method for various decision-making applications such as load frequency control. Fuzzy systems mimic the human reasoning behavior in which imprecise inputs are managed through IF-THEN

rules to realize a precise output. Fuzzy control structures have been employed as a new paradigm for automatic control succeeding the developing of fuzzy sets by L.A. Zadeh 1965 [44]. The fuzzy controller is treated as a nonlinear controller defined by linguistic rules such as big and small instead of differential equations. Consequently, the fuzzy control system exhibits remarkable performance with uncertain systems that embrace deficient or vague information regardless of the model of the system [29]. Fuzzy logic deposits the concept of infinite number of truth values manipulated between 0 and 1, unlike classical logic which has only two truth values, 0 or 1.

Two types of fuzzy logic controller exist, namely type 1 (T1FLC) and type 2 (T2FLC). T2FLC can deal with systems with more uncertainties to add more degrees of freedom to cope with the rapid varying uncertainties. T1FLC can be viewed as first-order approximation while T2FLC as second-order approximation of uncertainty [45,46]. T1FLC is mainly composed of four fundamental blocks, namely fuzzification, inference engine or mechanism, knowledge base, and defuzzification [47–49]. In T2FLC, an extra block is added called the type reducer to be inserted between the defuzzification stage and the inference stage [45].

Fuzzification is the conversion of the inputs from crisp values to linguistic variables. Each crisp input is assigned a degree to the fuzzy subset they belong via the membership function. The knowledge base contains the main rule which contains the IF-THEN fuzzy rules, as well as the database which contains the membership functions of the fuzzy sets. The inference mechanism is the decision-making part that performs the logic operations. Defuzzification is obtaining non fuzzy crisp output from the aggregate fuzzy set to be processed as a control signal. Various defuzzification methods such as Centroid Average, Maximum Center Average, and Bisector are used. The most common inference engines are Mamdani and Sugeno models. They are mainly different in the production stage, where Mamdani has an output membership function whereas Sugeno uses weighted average of the consequents to calculate the crisp output. The fuzzy inference process diagram is shown in Figure 4 [45].

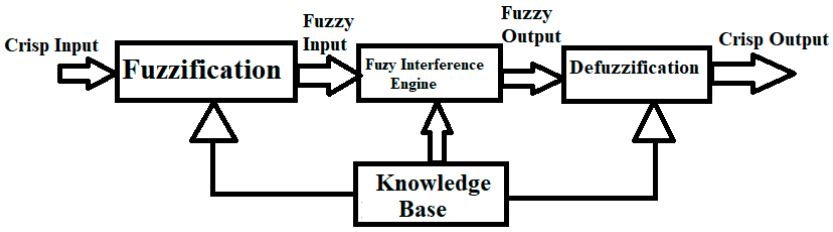

Figure 4. T1FLC inference process diagram.

Since a conventional PID controller possess linear characteristics, it fails to track fast and dynamic changes in widely spread nonlinear power systems. Accordingly, the integration of a PID controller with fuzzy logic as a hybrid controller can be an efficient solution to handle complex and nonlinear systems [45,46].

In our study, PI and PID controllers were implemented using a fuzzy control system to preserve the system frequency at its nominal value, which showed greater flexibility and adaptability to track the system rapid changes. The generalized architecture of the presented hybrid fuzzy controller is shown in Figure 5, where the system frequency error Δf, and the derivative of this error $d\Delta f$, are taken as inputs to the fuzzy controller. The hybrid fuzzy logic controller has one output that is continuously and online tuned to cope with any change in system frequency to acquire better dynamic and steady-state response. Based on the problem domain, input and output triangular membership functions were chosen for their simple and easy computation to generate the antecedents. Input membership functions are illustrated in Figure 6, with five linguistic variables, namely Negative Big (NB), Negative (N), Zero (Z), Positive (P), and Positive Big (PB), and twenty-five IF-THEN rules as shown in Table 2, while the output membership function is illustrated in Figure 6c. The

minimum-type implication method was utilized to produce the fuzzy consequents from the antecedents. Then, the maximum-type aggregation method was applied to obtain the output fuzzy set for each case. After that, the centroid method was used for defuzzification to generate the control signal that is applied to the governor of the turbine to increase or decrease the output generator frequency. The Mamdani fuzzy model was incorporated as the inference engine.

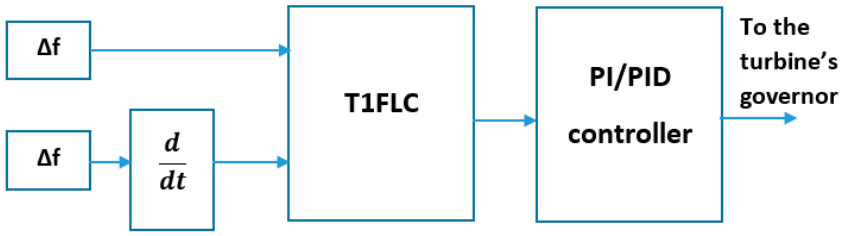

Figure 5. Block diagram of the fuzzy controller.

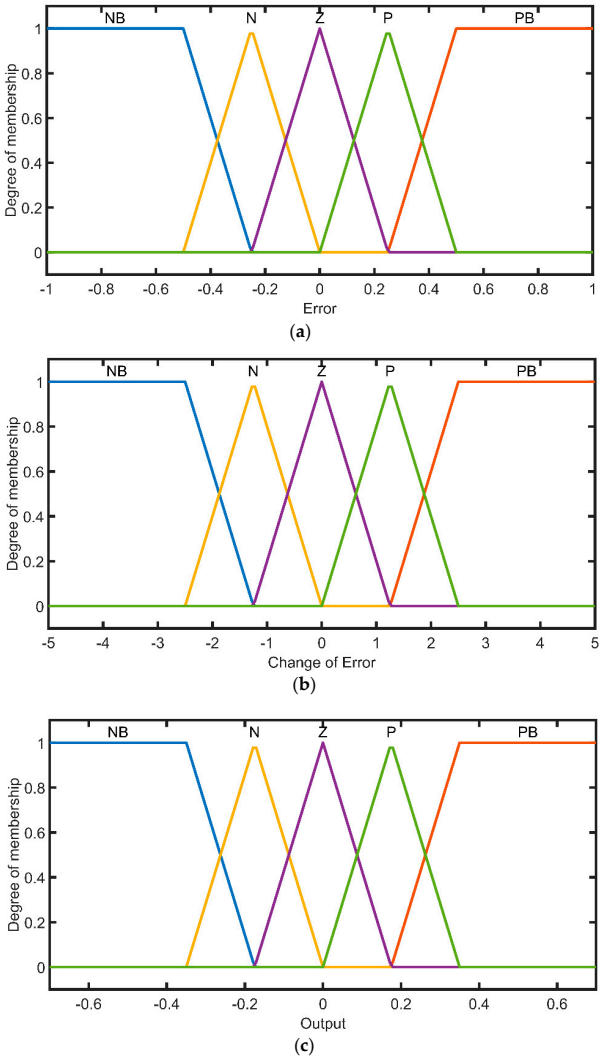

Figure 6. (**a**) The first input membership function. (**b**) The second input membership function. (**c**) Output membership function.

Table 2. Rules for the proposed controller.

		Error				
		NB	**N**	**Z**	**P**	**PB**
Change of Error	NB	NB	NB	NB	N	Z
	N	NB	NB	N	Z	P
	Z	NB	N	Z	P	PB
	P	N	Z	P	PB	PB
	PB	Z	P	PB	PB	PB

4. Results

The results are divided into two sections. In the first section, a single area system is presented where three test cases are studied. The first case is applying a step disturbance at t = 10 s, as shown in Figure 7. The proposed fuzzy EO PI controller is used and compared with a PI controller optimized once by a harmony search algorithm (HSA), once by a genetic algorithm (GA), and finally by a gravitational search algorithm (GSA), as presented in [42]. The second case is conducted by examining all the controllers used in case 1 against dynamic reference, as shown in Figure 8. Finally, in the third case, the proposed controller is examined without repeating the optimization against wind disturbance, as illustrated in Figure 9 and compared with the PI controller in [42], but the optimization is repeated.

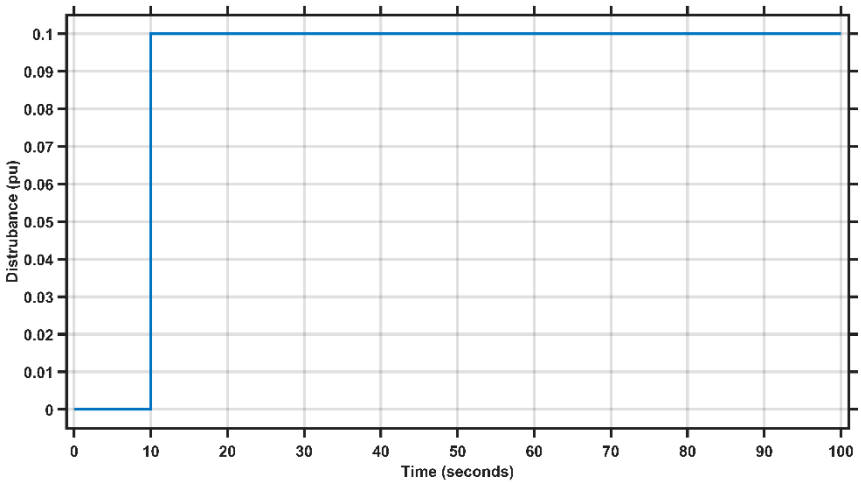

Figure 7. Step disturbance of case 1.

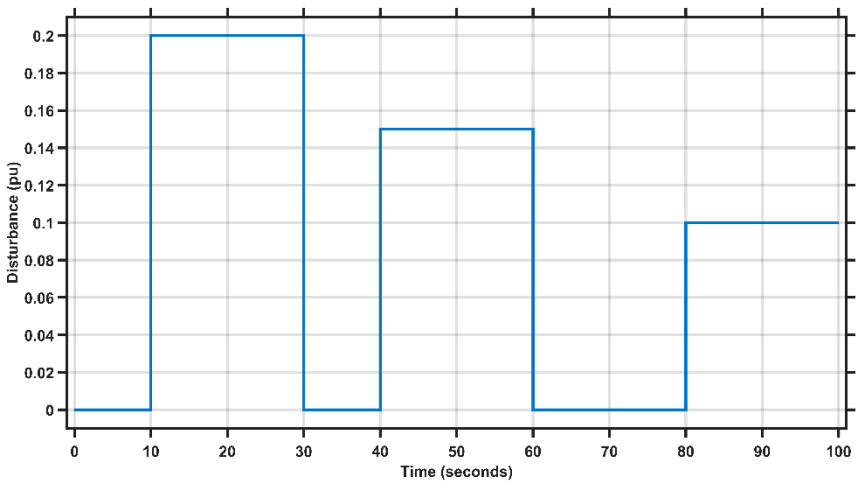

Figure 8. Dynamic disturbance of case 1.

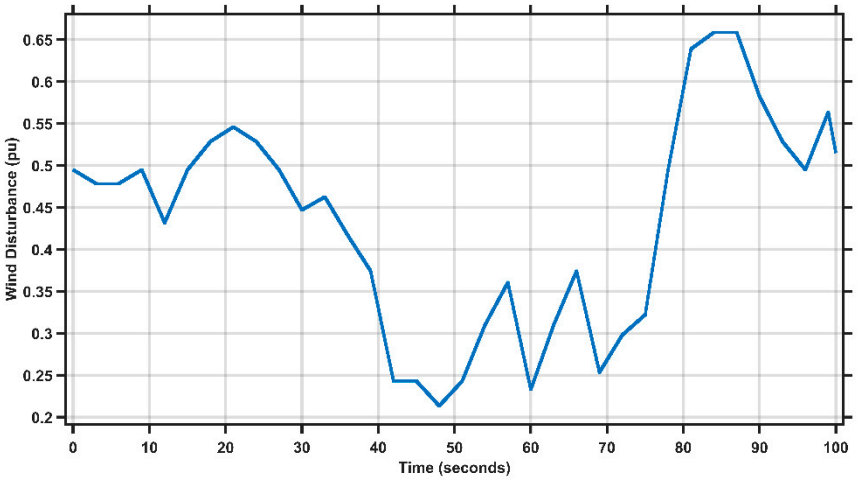

Figure 9. Wind disturbance.

In the second section, a two-area system is presented and two test cases are applied. In the first case, the proposed fuzzy EO PID controller is compared with the PIDA controller optimized by the harmony search algorithm (HSA), sine-cosine algorithm (SCA), and teaching-learning-based-optimization (TLBO) [50] under 1% disturbance in area 1. In the second case, the proposed fuzzy EO PID controller is compared with PIDA optimized by TLBO [50] under wave disturbance.

4.1. First Section

4.1.1. Case 1

The frequency deviation results of case 1, which has the step disturbance shown in Figure 7, are depicted in Figure 10.

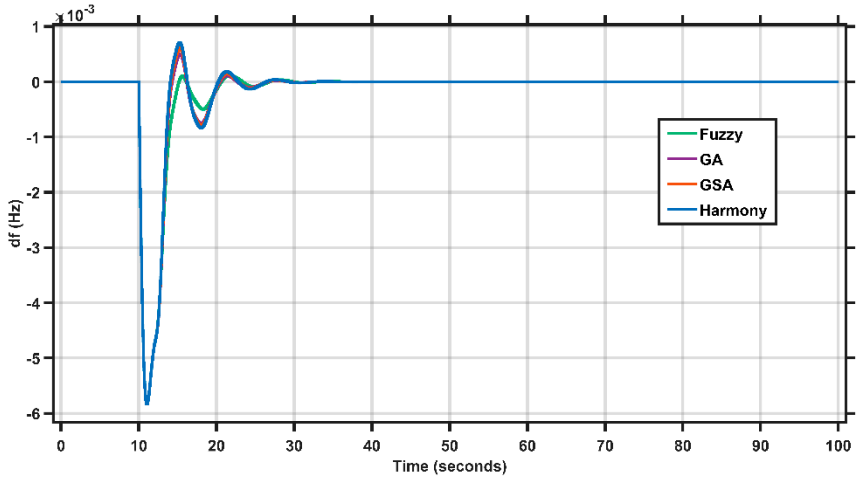

Figure 10. The frequency deviation under step disturbance.

Clearly, the proposed fuzzy EO PI has the lower overshoot with respect to PI-GA, PI-GSA, and PI-HSA, by 18.65%, 15.88%, and 13.556%. The proposed controller output signals are shown in Figure 11.

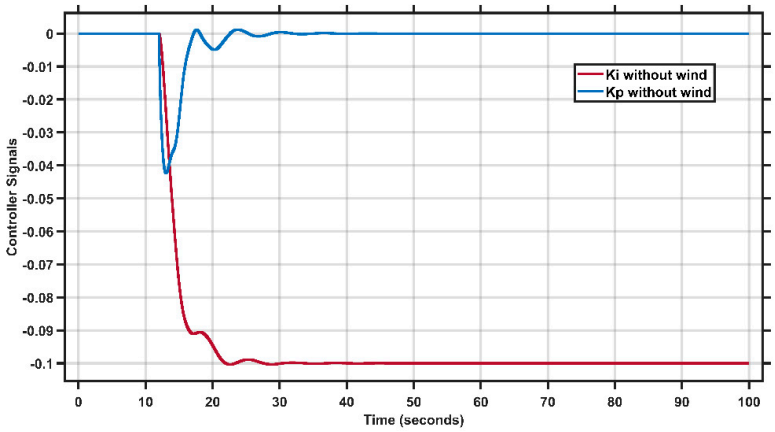

Figure 11. The output control signals of the fuzzy PI controller in case 1.

4.1.2. Case 2

The frequency deviation results of case 2, which has the dynamic disturbances of Figure 8, are shown in Figure 12.

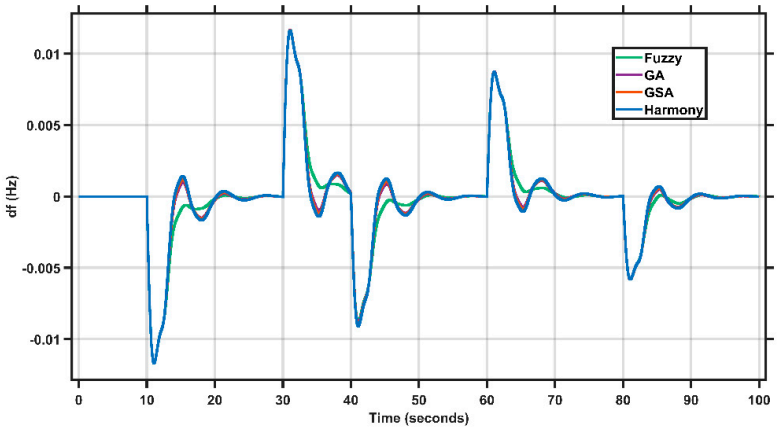

Figure 12. The frequency deviation under dynamic disturbance.

It is clear from Figure 12 that the proposed controller has the best dynamic performance over PI-GA, PI-GSA, and PI-HSA in [22]. The control signals of the proposed controller are shown in Figure 13.

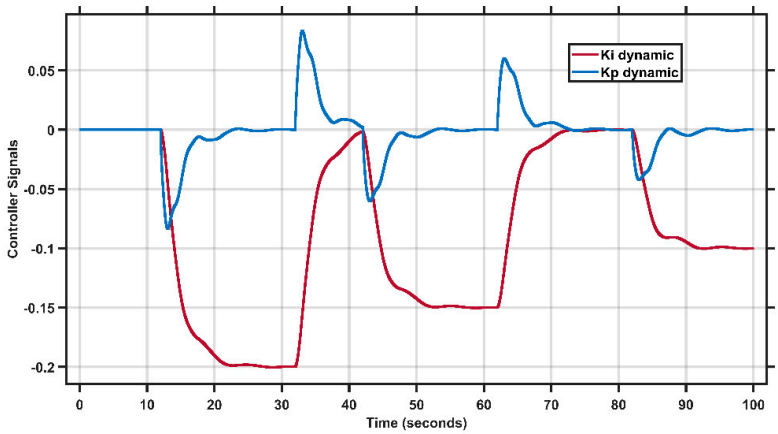

Figure 13. The output control signals of the fuzzy PI controller in case 2.

4.1.3. Case 3

The frequency deviation results of case 3, which has the wind disturbance shown in Figure 9 in addition to the step disturbance in Figure 7, are shown in Figure 14 and scoped in Figure 15.

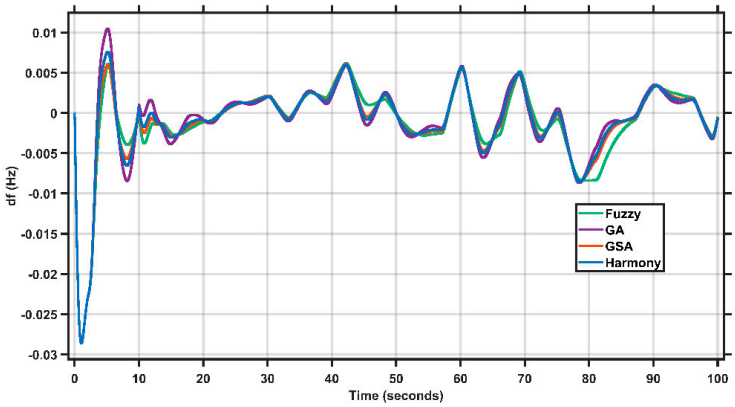

Figure 14. The frequency deviation under wind disturbance.

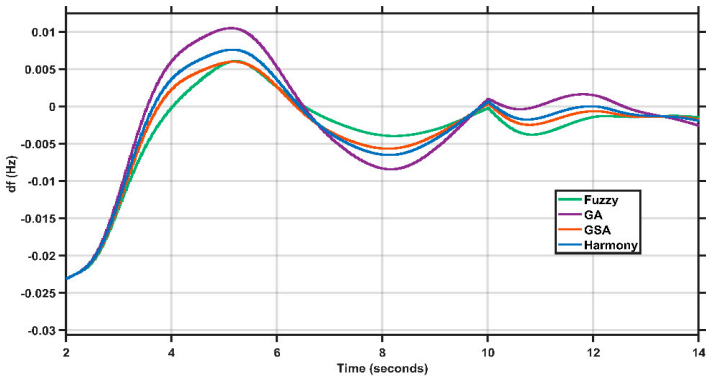

Figure 15. The scoped frequency deviation results under wind disturbance.

It is clear from Figures 14 and 15 that the proposed controller has the lowest overshoot and less oscillations than the methods presented in [22] without repeating the initialization. It is obvious that the peak-to-peak oscillation with the proposed controller is lower than PI-GA by 59%, PI-HSA by 47%, and PI-GSA by 30%. The proposed controller signals are shown in Figure 16.

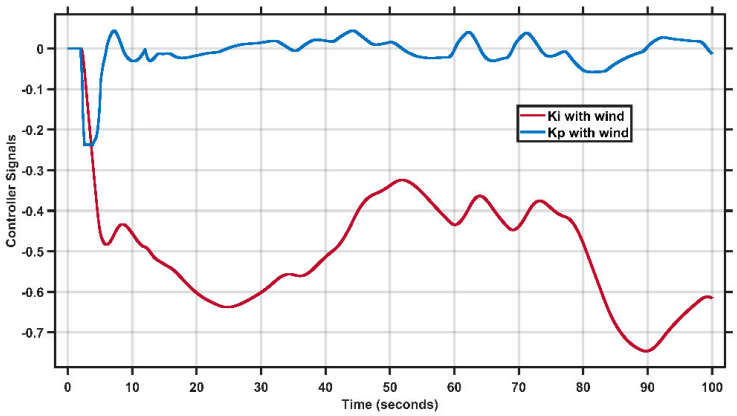

Figure 16. The proposed controller signals under wind disturbance.

The gains of the controllers in [42] and the initials of the proposed controller are presented in Tables 3 and 4.

Table 3. Gains of controller in case 1 and 2.

	Kp	Ki
Fuzzy EO PI initials	0.4922	0.3648
GA PI	0.4218	0.2928
GSA PI	0.432	0.299
HSA PI	0.4430	0.3043

Table 4. Gains of controller in case 3.

	Kp	Ki
Fuzzy EO PI initials	**Same initial gains of Case 1**	
GA PI	0.5469	0.3922
GSA PI	0.4846	0.3321
HAS PI	0.5085	0.3532

4.2. Second Section

The model under study in this section is the two-area system presented in [50], as shown in Figure 1b. Two cases are studied for the two-area system. In the first case, the loading of area 1 is varied by 1%, while the disturbance in case 2 is the wave energy disturbance presented in Figure 17.

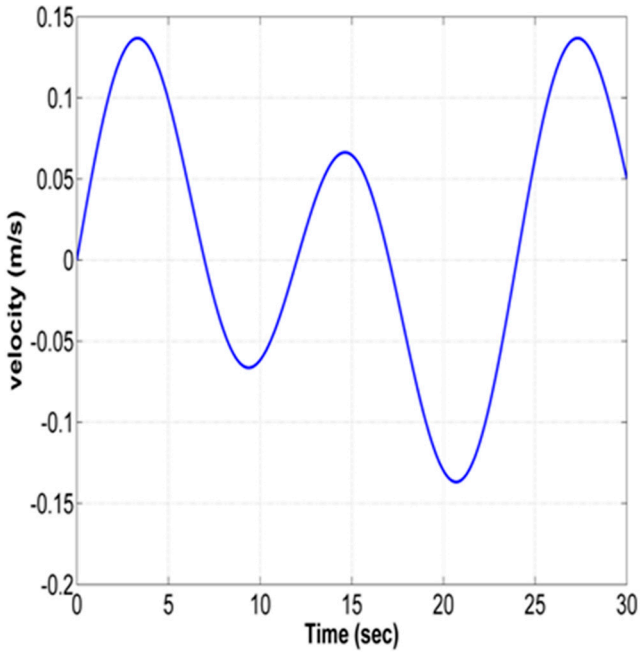

Figure 17. Wave disturbance.

4.2.1. Case 1

In this case, 1% load change at area 1 is applied. The change in area 1 frequency (df1), the change in area 2 frequency (df2), and the tie power (dP12) are shown in Figures 18–20.

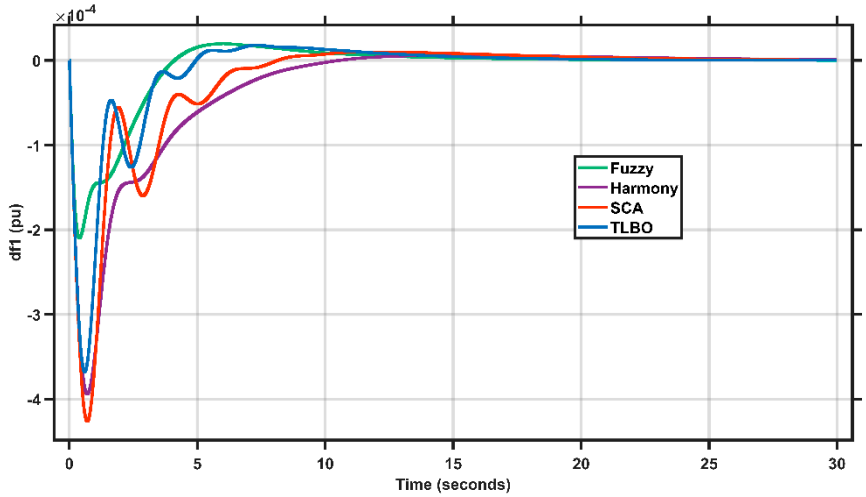

Figure 18. Change in area 1 frequency under 1% load change in area 1.

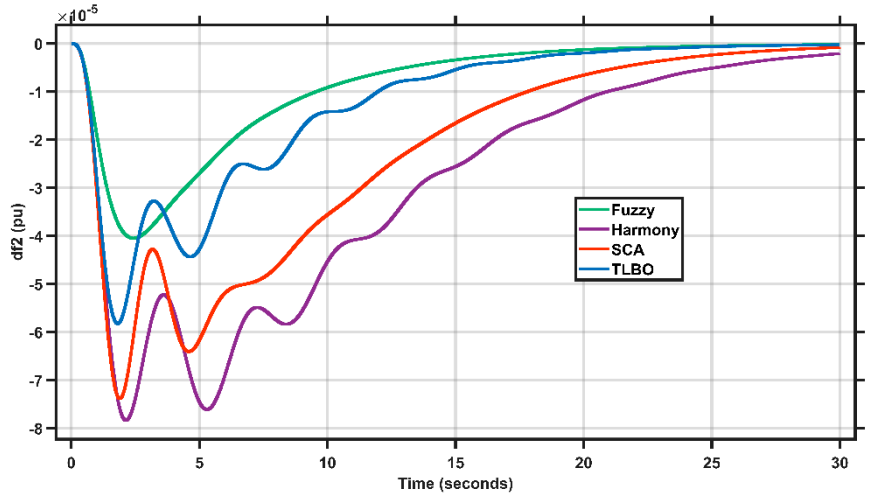

Figure 19. Change in area 2 frequency under 1% load change in area 1.

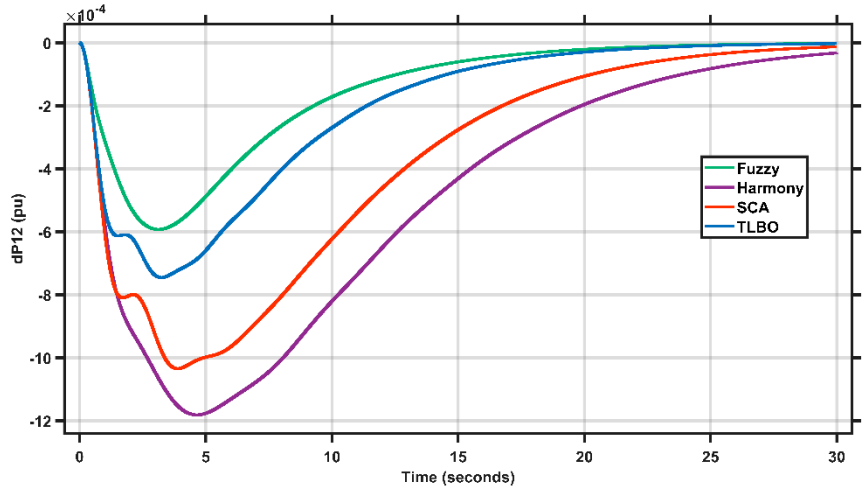

Figure 20. Change in power tie under 1% load change in area 1.

From Figures 18–20, it is evident that the overshoot with the proposed controller is lower than PIDA-HSA by 55%, PIDA-SCA by 50%, and PIDA-TLBO by 42% in df1, while in df2, the overshoot with the proposed controller is lower than PIDA-HS by 50%, PIDA-SCA

by 46%, and PIDA-TLBO by 28%. Finally in case of tie power, the overshoot with the proposed controller is lower than PIDA-HSA by 50%, PIDA-SCA by 40%, and PIDA-TLBO by 15%. Moreover, the proposed controller has more smoothing performance than the PIDA presented in [50].

4.2.2. Case 2

In this case, wave energy disturbance is applied to the system. The change in area 1 frequency (df1), the change in area 2 frequency (df2), and the tie power (dP12) are presented in Figures 21–23.

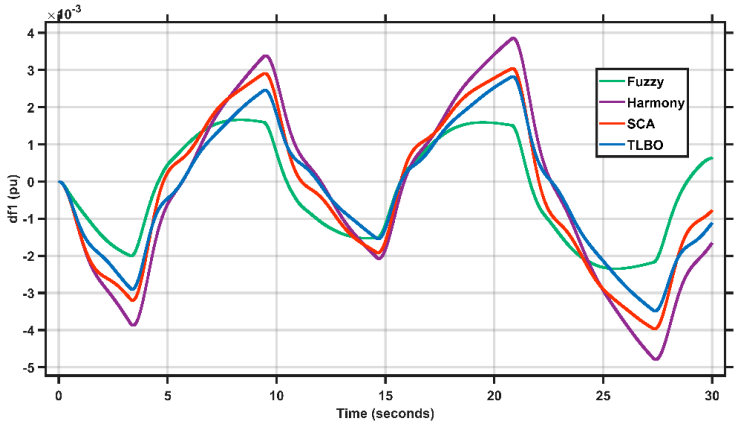

Figure 21. Change in area 1 frequency under wave disturbance.

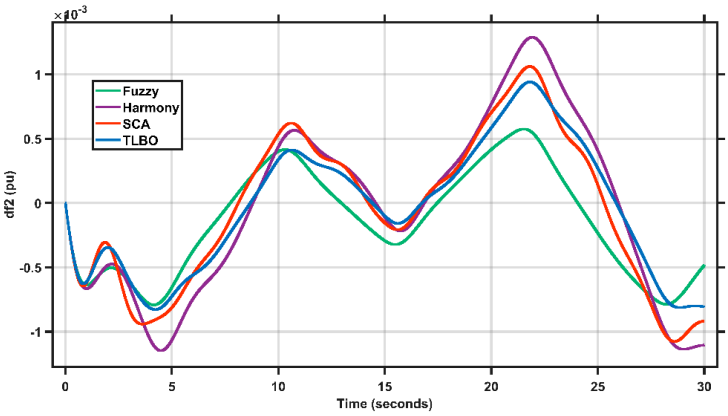

Figure 22. Change in area 2 frequency under wave disturbance.

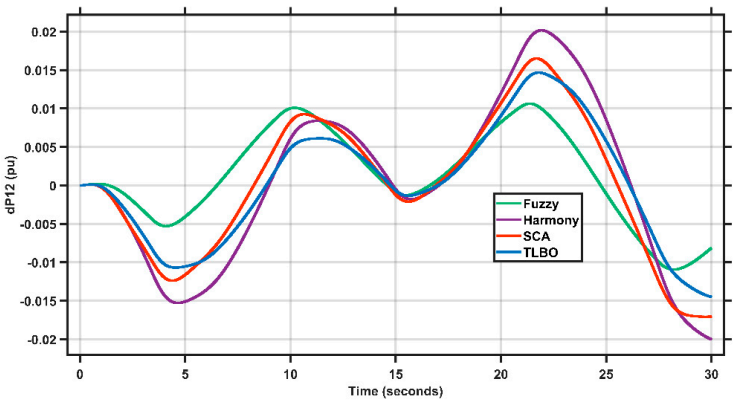

Figure 23. Change in tie power under wave disturbance.

From Figures 21–23, it is obvious that the peak-to-peak oscillation with the proposed controller is lower than PIDA-HSA by 50%, PIDA-SCA by 41%, and PIDA-TLBO by 30%

in df1. In df2, the peak-to-peak oscillation with the proposed controller is lower than PIDA-HS by 48%, PIDA-SCA by 35%, and PIDA-TLBO by 13%. Finally, in the case of tie power, the peak-to-peak oscillation with the proposed controller is lower than PIDA-HSA by 43%, PIDA-SCA by 23%, and PIDA-TLBO [50] by 20%.

5. Conclusions

A fuzzy PI/PID controller is proposed in this article to enhance the AGC system performance. The initialization of the controller gains was conducted by EO optimization. First, the validation of the proposed fuzzy PI controller was performed through comparison with PI-TLBO base, PI-HSA base, and PI-GSA base under step, dynamic, and wind generator disturbances in a single-area system. The proposed controller proved its superiority, where the system has better overshoot, dynamic performance, and less oscillations than the other methods. Moreover, the proposed controller proved its robustness through the auto-tuning of the gains. Finally, the proposed fuzzy PID controller also proved its superiority over the PIDA-TLBO, PIDA-SCA, and PIDA-HSA under step and wave energy disturbance in the two-area system.

Author Contributions: Conceptualization, S.M. and A.O.B.; methodology, M.A.A.; software, S.M.; validation, M.A.A., H.K. and E.E.; formal analysis, M.S.; investigation, M.A.A. and H.K.; resources, M.S.; data curation, A.O.B.; writing—original draft preparation, S.M., A.O.B., M.A.S. and H.K.; writing—review and editing, S.M., A.O.B., H.K. and M.A.S.; visualization, M.S. and E.E.; supervision, M.A.A. and H.K.; project administration, H.K. and E.E. All authors have read and agreed to the published version of the manuscript.

Funding: This research received no external funding.

Informed Consent Statement: Not applicable.

Data Availability Statement: Not applicable.

Conflicts of Interest: The authors declare no conflict of interest.

References

1. Çelik, E.; Durgut, R. Performance enhancement of automatic voltage regulator by modified cost function and symbiotic organisms search algorithm. *Eng. Sci. Technol. Int. J.* **2018**, *21*, 1104–1111. [CrossRef]
2. Mohanty, P.K.; Sahu, B.K.; Panda, S. Tuning and Assessment of Proportional–Integral–Derivative Controller for an Automatic Voltage Regulator System Employing Local Unimodal Sampling Algorithm. *Electr. Power Compon. Syst.* **2014**, *42*, 959–969. [CrossRef]
3. Mosaad, A.M.; Attia, M.A.; Almoataz, Y.A. Comparative Performance Analysis of AVR Controllers Using Modern Optimization Techniques. *Electr. Power Compon. Syst.* **2018**, *46*, 2117–2130. [CrossRef]
4. Ali, M.N.; Soliman, M.; Mahmoud, K.; Guerrero, J.M.; Lehtonen, M.; Darwish, M.M.F. Resilient Design of Robust Multi-Objectives PID Controllers for Automatic Voltage Regulators: D-Decomposition Approach. *IEEE Access* **2021**, *9*, 106589–106605. [CrossRef]
5. Köse, E. Optimal Control of AVR System with Tree Seed Algorithm-Based PID Controller. *IEEE Access* **2020**, *8*, 89457–89467. [CrossRef]
6. Peddakapu, K.; Mohamed, M.R.; Srinivasarao, P.; Veerendra, A.S.; Kishore, D.J.K.; Leung, P.K. Review on automatic generation control strategies for stabilizing the frequency deviations in multi-area power system. *Int. J. Ambient. Energy* **2021**, 1–24. [CrossRef]
7. Kumar, P.; Kothari, D.P. Recent Philosophies of Automatic Generation Control Strategies in Power Systems. *IEEE Trans. Power Syst.* **2005**, *20*, 346–357.
8. Shayeghi, H.; Shayanfar, H.A.; Jalili, A. Load Frequency Control Strategies: A State-of-the-Art Survey for the Researcher. *Energy Convers. Manag.* **2009**, *50*, 344–353. [CrossRef]
9. Pandey, S.K.; Mohanty, S.R.; Kishor, N. A Literature Survey on Load–Frequency Control for Conventional and Distribution Generation Power Systems. *Renew. Sustain. Energy Rev.* **2013**, *25*, 318–334. [CrossRef]
10. Bakken, H.B.; Grande, O.S. Automatic Generation Control in a Deregulated Power System. *IEEE Trans. Power Syst.* **1998**, *13*, 1401–1406. [CrossRef]
11. Mokhtar, S.; Anayi, F. TLBO Tuned a Novel Robust Fuzzy Control Structure for LFC of a Hybrid Power System with Photovoltaic Source. *Eng. Proc.* **2022**, *19*, 1.
12. Nanda, J.; Mishra, S.; Saikia, L.C. Maiden application of bacterial foraging-based optimization technique in multiarea automatic generation control. *IEEE Trans Power Syst* **2009**, *24*, 602–609. [CrossRef]

13. Nanda, J.; Kaul, B.L. Automatic generation control of an interconnected power system. *Proc. Inst. Electr. Eng.* **1978**, *125*, 385–390. [CrossRef]
14. Hari, L.; Kothari, M.L.; Nanda, J. Optimum selection of speed regulation parameters for automatic generation control in discrete mode considering generation rate constraints. *IEE Proc. C—Gener. Transm. Distrib.* **1991**, *138*, 401–406. [CrossRef]
15. Nanda, J.; Mangla, A.; Suri, S. Some new findings on automatic generation control of an interconnected hydrothermal system with conventional controllers. *IEEE Trans. Energy Convers.* **2006**, *21*, 187–194. [CrossRef]
16. Daraz, A.; Malik, S.A.; Haq, A.U. Review of Automatic Generation Control for Multi-Source Interconnected Power System Under Deregulated Environment. In Proceedings of the 2018 International Conference on Power Generation Systems and Renewable Energy Technologies (PGSRET), Barcelona, Spain, 10–12 September 2018; pp. 1–5. [CrossRef]
17. Panda, S.; Padhy, N.P. Comparison of particle swarm optimization and genetic algorithm for FACTS-based controller design. *Appl. Soft Comput.* **2008**, *8*, 1418–1427. [CrossRef]
18. Miavagh, F.M.; Miavaghi, E.A.A.; Ghiasi, A.R.; Asadollahi, M. Applying of PID, FPID, TID and ITID controllers on LFC using particle swarm optimization (PSO). In Proceedings of the 2015 2nd International Conference on Knowledge-Based Engineering and Innovation (KBEI), Tehran, Iran, 5–6 November 2015; pp. 866–871.
19. Kumari, S.; Shankar, G.; Prince, A. Load Frequency Control Using Linear Quadratic Regulator and Differential Evolution Algorithm. In Proceedings of the 2016 International Conference on Next Generation Intelligent Systems (ICNGIS), Kottayam, India, 1–3 September 2016.
20. Omer, M.; Soliman, M.; Ghany, A.M.A.; Bendary, F. Ant colony optimization based PID for single area load frequency control. In Proceedings of the 2013 5th International Conference on Modelling, Identification and Control (ICMIC), Cairo, Egypt, 31 August–2 September 2013.
21. Morsali, J.; Zare, K.; Hagh, M.T. A novel dynamic model and control approach for SSSC to contribute effectively in AGC of a deregulated power system. *Int. J. Electr. Power Energy Syst.* **2018**, *95*, 239–253. [CrossRef]
22. Sahu, B.K.; Pati, S.; Panda, S. Hybrid differential evolution particle swarm optimization optimized fuzzy proportional–integral derivative controller for automatic generation control of interconnected power system. *IET Gener. Transm. Distrib.* **2014**, *8*, 1789–1800. [CrossRef]
23. Gozde, H.; Taplamacioglu, M.C. Automatic generation control application with craziness-based particle swarm optimization in a thermal power system. *Int. J. Electr. Power Energy Syst.* **2011**, *33*, 8–16. [CrossRef]
24. Ali, E.S.; Abd-Elazim, S.M. Bacteria foraging optimization algorithm-based load frequency controller for interconnected power system. *Int. J. Electr. Power Energy Syst.* **2011**, *33*, 633–638. [CrossRef]
25. Rout, U.K.; Sahu, R.K.; Panda, S. Design and analysis of differential evolution algorithm based automatic generation control for interconnected power system. *Ain. Shams. Eng. J.* **2013**, *4*, 409–421. [CrossRef]
26. Yesil, E.; Guzelkaya, M.; Eksin, I. Self tuning fuzzy PID type load and frequency controller. *Energy Convers. Manag.* **2004**, *45*, 377–390. [CrossRef]
27. Khuntia, S.R.; Panda, S. Simulation study for automatic generation control of a multi-area power system by ANFIS approach. *Appl. Soft Comput.* **2012**, *12*, 333–341. [CrossRef]
28. Ghosal, S.P. Optimization of PID gains by particle swarm optimization in fuzzy based automatic generation control. *Electr. Power Syst. Res.* **2004**, *72*, 203–212. [CrossRef]
29. Kumar, N.; Chelliah, T.R.; Srivastava, S.P. Analysis of doubly fed induction machine operating at motoring mode subjected to voltage sag. *Eng. Sci. Technol. Int. J.* **2016**, *19*, 1117–1131. [CrossRef]
30. Kaundal, V.; Mondal, A.K.; Sharma, P.; Bansal, K. Tracing of shading effect on underachieving SPV cell of an SPV grid using wireless sensor network. *Eng. Sci. Technol. Int. J.* **2015**, *18*, 475–484. [CrossRef]
31. Nayanar, V.; Kumaresan, N.; Gounden, N.G.A. Wind-driven SEIG supplying DC microgrid through a single-stage power converter. *Eng. Sci. Technol. Int. J.* **2016**, *19*, 1600–1607.
32. Attia, M.A.; Hany, M.H.; Abdelaziz, A.Y. Performance enhancement of power systems with wave energy using gravitational search algorithm based TCSC devices. *Eng. Sci. Technol. Int. J.* **2016**, *19*, 1661–1667. [CrossRef]
33. Alzaareer, K.; Al-Shetwi, A.Q.; El-bayeh, C.Z.; Taha, M.B. Automatic generation control of multi-area interconnected power systems using ANN controller. *Rev. D'intelligence Artif.* **2020**, *34*, 1–10. [CrossRef]
34. Kumar, A.; Singh, O. Recent Strategies for Automatic Generation Control of Multi-Area Interconnected Power Systems. In Proceedings of the 2019 3rd International Conference on Recent Developments in Control, Automation & Power Engineering (RDCAPE), Noida, India, 10–11 October 2019; pp. 153–158. [CrossRef]
35. Muntasir, A.M.; Alquthami, T. Optimal Design of Automatic Generation Control Based on Simulated Annealing in Interconnected Two-Area Power System Using Hybrid PID—Fuzzy Control. *Energies* **2022**, *15*, 1540. [CrossRef]
36. Maroufi, O.; Choucha, A.; Chaib, L. Hybrid fractional fuzzy PID design for MPPT-pitch control of wind turbine-based bat algorithm. *Electr. Eng.* **2020**, *102*, 2149–2160. [CrossRef]
37. Mahto, T.; Malik, H.; Mukherjee, V.; Alotaibi, M.A.; Almutairi, A. Renewable generation-based hybrid power system control using fractional order-fuzzy controller. *Energy Rep.* **2021**, *7*, 641–653.
38. Asgharnia, A.; Shahnazi, R.; Jamali, A. Performance and robustness of optimal fractional fuzzy PID controllers for pitch control of a wind turbine using chaotic optimization algorithms. *ISA Trans.* **2018**, *79*, 27–44. [CrossRef] [PubMed]

39. Yang, L.; Sun, Q.; Zhang, N.; Li, Y. Indirect Multi-Energy Transactions of Energy Internet With Deep Reinforcement Learning Approach. *IEEE Trans. Power Syst.* **2022**, *37*, 4067–4077. [CrossRef]
40. Xi, L.; Zhang, L.; Xu, Y.; Xu, Y.C. Automatic Generation Control Based on Multiple-step Greedy Attribute and Multiple-level Allocation Strategy. *CSEE J. Power Energy Syst.* **2022**, *8*, 281–292. [CrossRef]
41. Yushuai, L.; Zhang, H.; Liang, X.; Huang, B. Event-triggered-based distributed cooperative energy management for multienergy systems. *IEEE Trans. Ind. Inform.* **2018**, *15*, 2008–2022.
42. Attia, M.A.; Mokhtar, M.; Abdelaziz, A.Y.; Sasis, S.; Kumar, S.; Saket, R.K. Optimal Controller Design for Automatic Generation Control Under Renewable Energy Disturbance. In *Advances in Smart Grid Automation and Industry 4.0*; Springer: Singapore, 2021; pp. 121–132.
43. Faramarzi, A.; Heidarinejad, M.; Stephens, B.; Mirjalili, S. Equilibrium optimizer: A novel optimization algorithm. *Knowl.-Based Syst.* **2020**, *191*, 105190. [CrossRef]
44. Jäkel, J.; Mikut, R.; Bretthauer, G. *Fuzzy Control Systems*. Institute of Applied Computer Science; Forschungszentrum Karlsruhe GmbH: Karlsruhe, Germany, 2004.
45. Kumar, A.; Kumar, V. Performance analysis of optimal hybrid novel interval type-2 fractional order fuzzy logic controllers for fractional order systems. *Expert Syst. Appl.* **2018**, *93*, 435–455. [CrossRef]
46. Laib, A.; Talbi, B.; Gharib, A.K.M. Hybrid Interval Type-2 Fuzzy PID+I Controller for a Multi-DOF Oilwell Drill-String System. *IEEE Access* **2022**, *10*, 67262–67275. [CrossRef]
47. Khan, A.A.; Rapal, N. Fuzzy PID Controller: Design, Tuning and Comparison with Conventional PID Controller. In Proceedings of the 2006 IEEE International Conference on Engineering of Intelligent Systems, Islamabad, Pakistan, 22–23 April 2006; pp. 1–6. [CrossRef]
48. Gheisarnejad, M. An effective hybrid harmony search and cuckoo optimization algorithm based fuzzy PID controller for load frequency control. *Appl. Soft Comput.* **2018**, *65*, 121–138. [CrossRef]
49. Annapoorani, K.I.; Rajaguru, V.; Padmanabhan, S.A.; Kumar, K.M.; Venkatachalam, S. Fuzzy logic-based integral controller for load frequency control in an isolated micro-grid with superconducting magnetic energy storage unit. *Mater. Today Proc.* **2022**, *58*, 244–250. [CrossRef]
50. Elsaied, M.M.; Attia, M.A.; Mostafa, M.A.; Mekhamer, S.F. Application of Different Optimization Techniques to Load Frequency Control with WECS in a Multi-Area System. *Electr. Power Compon. Syst.* **2018**, *46*, 739–756. [CrossRef]